FATIGUE CRACK GROWTH BEHAVIOR IN 6061-T6 ALUMINUM ALLOY WELDS OBTAINED BY MIEA

R.R. Ambriz[1,2,3,4], G. Mesmacque[1,2,3], A. Benhamena[1,2,3], A. Ruiz[4], A. Amrouche[1,2,3], V. H. López[4]

[1] Université Lille Nord de France, F-59000 Lille, France. [2] USTL, LML, F-59650 Villeneuve d'Ascq, France. [3] CNRS, UMR 8107, F-59650 Villeneuve d'Ascq.
E-mail: ricraf74@gmail.com

[4] Instituto de Investigaciones Metalúrgicas, Universidad Michoacana de San Nicolás de Hidalgo, A.P. 888, C.P. 58000, Morelia Michoacán, México.
E-mail: alruiz@umich.mx

ABSTRACT

This work reports the results of the fatigue crack growth on 6061-T6 aluminium alloy welds obtained by modified indirect electric arc (MIEA). Fatigue crack growth behavior in base metal, weld metal and heat affected zone (HAZ) of the welded joint was performed by means of compact-type (CT) specimens. Experimental results indicate that the fatigue crack length depends of the mechanical properties of the material. In this context it has been observed that the HAZ tends to delay the crack growth with respect to base metal and weld metal, this aspect is attributed to the larger plastic zone formed around the crack tip which is promoted by the microstructural transformation from β'' to β' precipitates. Also, has been found that the crack growth and stress intensity factor (ΔK) adjust with good confidence according to Paris law; however when ΔK reaches a critical value ~ 15 MPa $m^{1/2}$, the fatigue crack growth presents an important change which is related to the microstructural condition of the materials. Finally, the surfaces fractures analysis revealed interesting characteristics in terms of crack propagation.

KEYWORDS: Fatigue; crack growth; welding, 6061-T6.

1. INTRODUCTION.

The 6061-T6 aluminium alloy have a wide use in different fields like the automotive, railroad, chemical and oil industries. The main applications of this alloy are related to the high strength to weight ratio which makes them suitable for: structural parts for trucks, railroad cars, pressure vessels, pipelines, marine applications and mechanical components for machines. The most important characteristic of these alloy is that it can be solution treated and artificially aged to improve their mechanical properties ($\sigma_u \cong 310$ MPa) [1, 2]. The metallurgical characteristics and mechanical properties of the HAZ of 6061-T6 welded joints where studied by Malin [3] who found a correlation between thermal cycles microhardness profiles, failure location and tensile properties. Microhardness profiles along the width of the welds revealed that the failure of the tensile specimens consistently occurred in the softest area of the HAZ, where the temperatures experienced in the parent metal induced detrimental changes in the microstructure of the alloy. Thus, it is well known that fusion welding of 6061-T6 aluminium alloy leads to a significant loss of mechanical strength. In recent years, a novel joint design named Modified Indirect Electric Arc (MIEA) was envisaged and used to weld 6061-T6 [4] and 2014-T6 [5] aluminium plates with the gas metal arc welding process (GMAW). This joint is an interesting alternative to improve the mechanical properties and microstructural characteristics of these alloys, since only a single welding pass is required to weld plates of 12.7 mm in thickness, reducing thus the heat input during welding which in turn reduces the microstructural transformations in the HAZ and enhances the mechanical properties of the welded joints. In terms of fatigue behaviour, the effect of the welding profile in MIEA 6061-T6 aluminium alloy welds has been reported [6]. In this study the calculations are based on the effect of the stress concentration factor produced by the characteristic geometry of the welding profile formed after welding process. It was found that the fatigue life of welded samples using this welding technique was larger in comparison with data reported in the literature. Also, it was observed that there is a good correlation (R^2=0.90) between experimental and theoretical prediction according to Basquin's equation.

This study presents the experimental results of the fatigue crack growth in the base metal (BM), weld metal and heat affected zone (HAZ) of the 6061-T6 welded joints obtained by MIEA. Results are discussed in terms of growth and propagation of the cracks.

2. EXPERIMENTAL PROCEDURE.

Plates of 6061-T6 aluminum alloy with dimensions of 150 × 70 × 9.5 mm were joined by means of the MIEA welding technique [7]. GMA welding of the plates was performed using a constant-voltage power source of 300 A with a voltage range of 0 to 50 V. An ER4043 filler wire of 1.2 mm in diameter was fed at 145 mm s^{-1} with direct current-electrode positive (DCEP) along with Ar shielding gas flowing at 23.6 L min^{-1}. The torch was displaced at 3.6 mm s^{-1} and voltage (24 V) and current (230 A) were adjusted to produce a spray transfer mode with a visible stick out of 9 mm. Figure 1, shows the schematic representation of the MIEA welds.

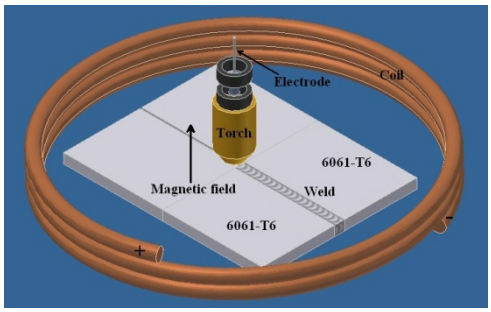

Figure 1. Schematic representation of MIEA welds.

First of all, tensile properties for the as-received 6061-T6 plates (longitudinal direction), weld metal and HAZ were evaluated. Tensile specimens were machined with the dimensions and geometry as specified by the ASTM B557-06 designation. The quasi-static tension test was performed with a head speed displacement of 0.0166 mm s^{1}. Deformation of the tensile specimens was measured with an Instron® extensometer model 2620-601.

Fatigue crack growth test in standard compact-type (CT) specimens was carried out in the base metal, weld metal and HAZ of the MIEA welded joints (Figure 2). Figure 3, shows the specimen dimensions according to ASTM E647-08 designation. For the crack growth test a constant amplitude cyclic loading with a sinusoidal wave form at a frequency of 20 Hz, load ratio R=0.1 and load range ΔP=2.5 kN were applied in atmospheric air at room temperature. The propagation of the crack was follow by means of a digital camera attached to a monitor. The crack growth a, as a function of number of cycles N, was represented by means of a-N graph and the crack growth rate da/dN, was presented graphically as a function of the stress intensity factor range ΔK (equation 1).
Finally, examination of the fractured surfaces of CT specimens was performed in the scanning electron microscope (SEM) in order to characterize the type of fracture and obtain insight into the failure mechanisms.

$$\Delta K = \frac{\Delta P(2+\alpha)}{B\sqrt{W}(1-\alpha)^{3/2}} \left(0.886 + 4.64\alpha - 13.32\alpha^2 + 14.72\alpha^3 - 5.6\alpha^4\right) \quad \alpha = \frac{a}{W} \tag{1}$$

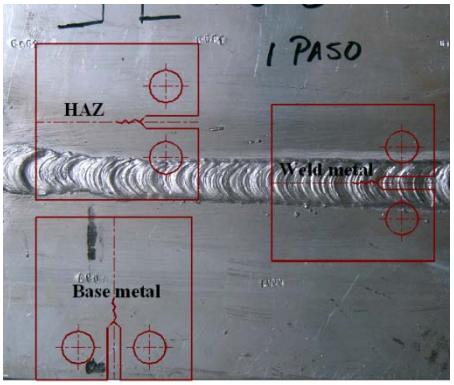

Figure 2. Welded joint and compact-type specimen.

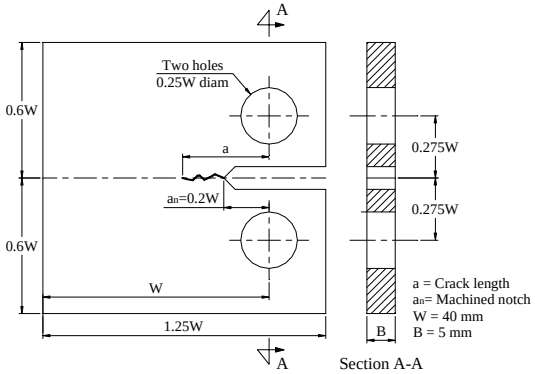

Figure 3. Standard compact-type specimen, CT.

3. RESULTS AND DISCUSSION

3.1. Tensile Behavior.

The individual mechanical behavior of the base metal, weld metal and HAZ, is shown in Figure 4 as a stress function of strain graph.

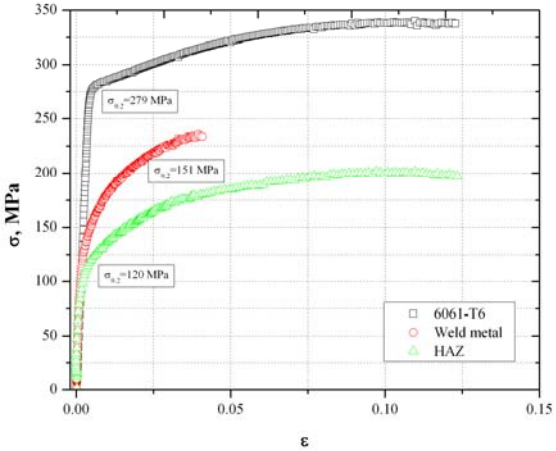

Figure 4. True stress-strain curves for as-received 6061-T6 plates, weld metal and HAZ condition.

It can be observed that the experimental results for the base metal are in agreement with nominal values found in the literature for 6061-T6 alloy [8]. Also, the base metal exhibits the best mechanical properties and the well-defined proportional limit. The tensile properties of the sample obtained from the HAZ presents a 41 % and a 19 % reduction of the ultimate strength with respect to the base metal and weld metal respectively. The loss of mechanical strength, commonly referred to as over-aging, when welding a 6061-T6 alloy is a fairly well-understood phenomenon and it is explained in terms of the precipitation sequence undergone by this alloy with temperature [9]. In a 6061 alloy, the T6 heat-treatment yields an aluminum matrix, α, in which very fine precipitates with needle shape, β", are homogeneously dispersed. However, during the welding process, the base metal adjacent to the fusion line is subjected to a gradient of temperature imposed by the welding thermal cycle. It causes the coarsening of β'' and its transformation into β' type precipitates the mechanism responsible of the decrease in hardening of the α matrix due to the incoherence of the β' phase caused by the thermodynamic instability of β'' in a welding process [10]. Although the weld metal shows higher tensile properties than the HAZ, during the tension test, the weld metal and the HAZ show the same behavior, i.e. both present a gradual transition from the elastic region to the plastic region. The weld metal exhibits, however, lower ductility caused by the high content of Si of the filler metal which, when mixing with the melted base metal, leads to a microstructure crowded of eutectic silicon which is a brittle phase that adversely affects the mechanical properties of the weld. The three samples have the same Young's modulus. A best fitting in the elastic region was performed and a value of E = 68 GPa was obtained.

3.2. Fatigue Crack Growth.

Figure 5 shows the general characteristics of the crack growth for the base metal, weld metal and HAZ. It is possible to observe that the propagation of the crack is nearly perpendicular to the applied load. Also, we can observe that the maximum displacement in function of the crack propagation is presented in the HAZ specimen, which is attributed to the mechanical properties and microstructural condition of the material.

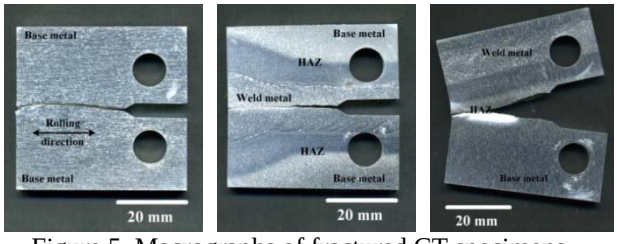

Figure 5. Macrographs of fractured CT specimens.

Fatigue crack growth as a function of number of cycles is shown in Figure 6. In this graph we can note that the fatigue crack length depends fundamentally of the tensile strength of material. In this sense we can observed that the HAZ tends to delay the crack growth in relation to base metal and weld metal. This behavior can be explained in function of the plastic zone formation (ductility) formed around the crack tip which tends to be larger than the base metal and weld metal (Figure 5). This plastic zone is promoted by the loss of hardening in the welded joint due to the microstructural transformation of very fine precipitates with needle shape β", to coarse precipitates with bar shape β', formed after a fusion welding process. Thus, when the crack reaches a critical value, it tends to propagate very quickly in a similar manner to the base metal.

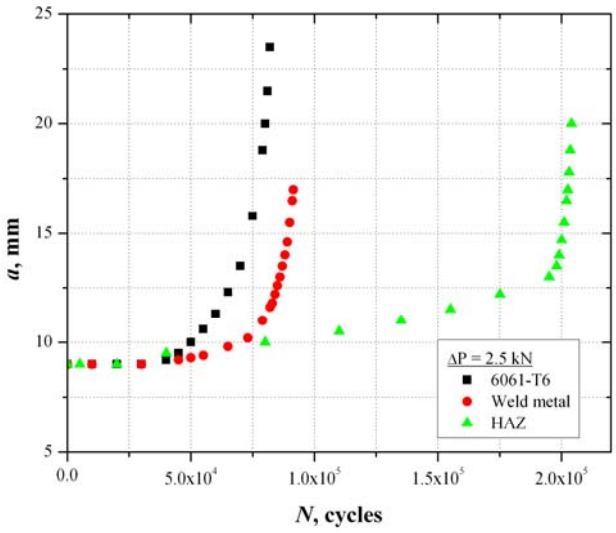

Figure 6. Crack length vs. cycles data for base metal (6061-T6), weld metal and HAZ.

The experimental data of da/dN versus ΔK are show in Figure 7. These results were fitted according to the Paris law:

$$\frac{da}{dN} = C(\Delta K)^n \qquad (2)$$

where C and n are experimental values obtained from fitting curve. Table 1, summaries these values and the correlation factor R^2. The resulting experimental curve and the prediction model are also shown in Figure 7.

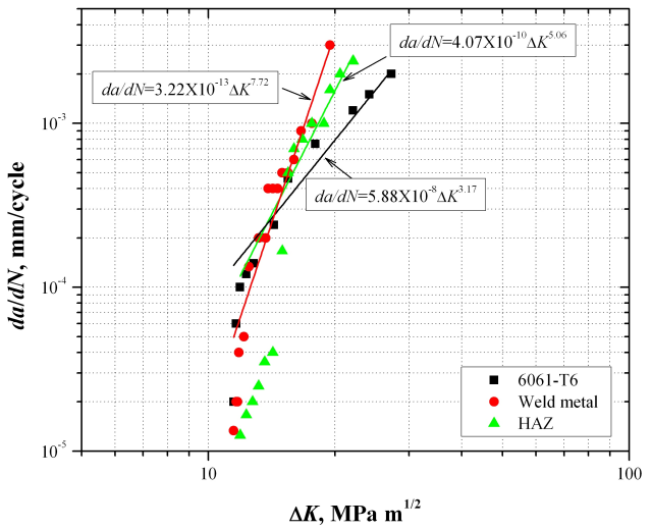

Figure 7. Fatigue crack growth rate for base metal (6061-T6), weld metal and HAZ.

Table 1. Experimental values from fitting curve.

Material	***C***	***n***	***R^2***
6061-T6	5.88×10^{-8}	3.17	0.97
Weld	3.22×10^{-13}	7.72	0.97
ZAT	4.07×10^{-10}	5.06	0.95

From Figure 7, we can see that there is a good correlation between experimental and theoretical predictions, independently of the mechanical properties and microstructure of the welded joint. However, it should be noted an important difference between *da/dN* versus ΔK behavior. It means that the crack growth behavior is divided by a critical stress intensity factor, ΔK_{crit} ~ 15 MPa $m^{1/2}$. Nevertheless, when ΔK_{crit}< 15 MPa $m^{1/2}$ the faster crack growth correspond to the base metal, followed by the weld metal and the HAZ. In contrast, when ΔK_{crit} > 15 MPa $m^{1/2}$ the crack growth in the base metal is the slowest. Also, is possible to observe that the crack propagation in the weld metal has the maximum crack growth rate, which is attributed to the brittle microstructure produced after welding process (see Figure 4).

3.3. Fracture Modes.

Figure 8, shows the general features of surfaces fractures for base metal, weld metal and HAZ. In these micrographs is possible to identify a pre-crack zone with a width of roughly 1 mm, as well as the different stages of fatigue failure mechanism, especially the path propagation of the fracture characterized by river patterns and the transition of propagation and failure zones. In this context we can note the flat fracture surface presented by the weld metal and HAZ, in contrast to the surface fracture of the base metal.

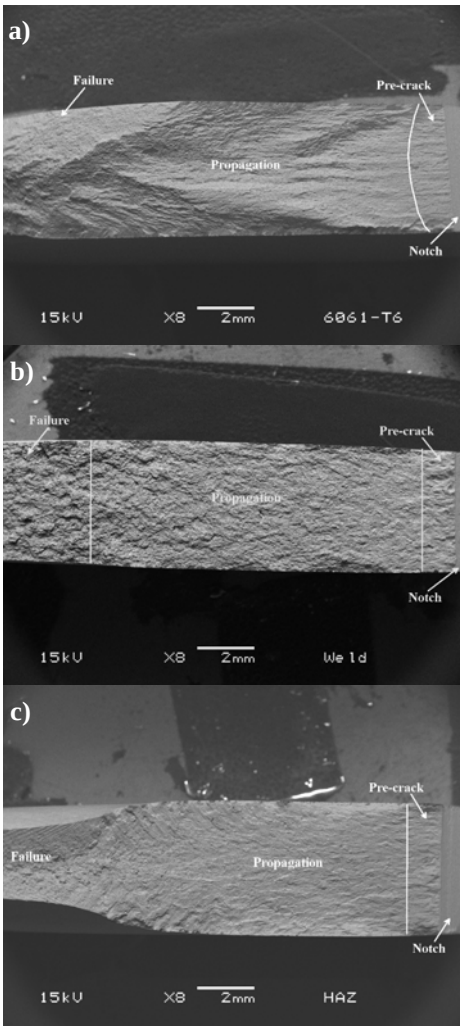

Figure 8. General view of surface fractures, a) base metal, b) weld metal and c) HAZ.

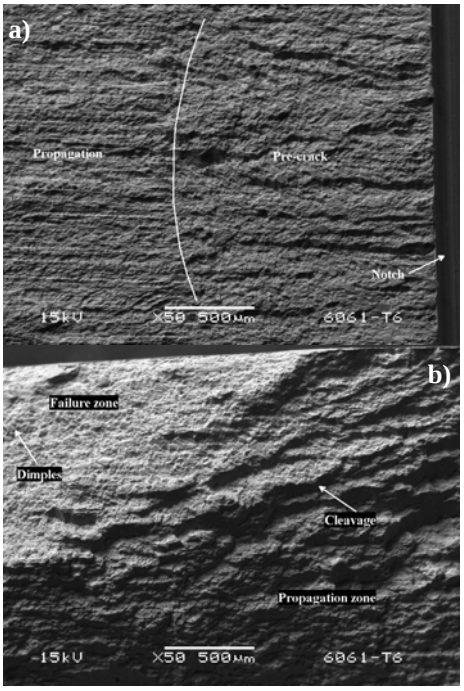

Figure 9. Details of base metal fracture, a) pre-crack and propagation and b) propagation and failure.

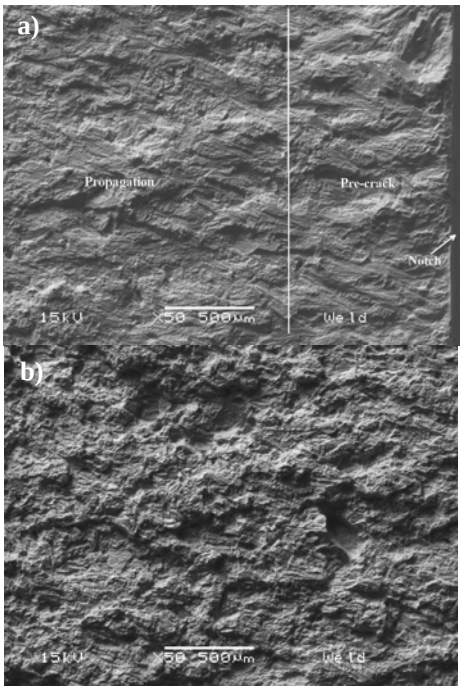

Figure 10. Details of weld metal surface fracture, a) pre-crack and propagation and b) failure.

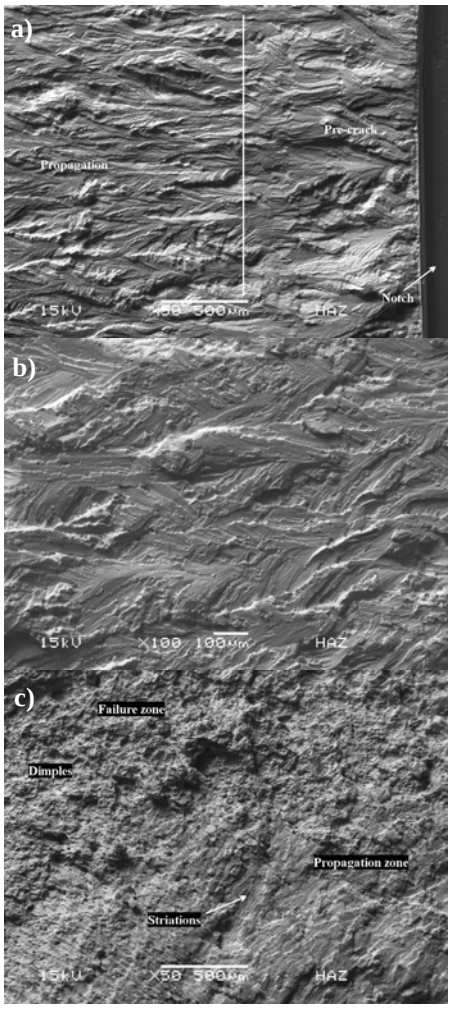

Figure 11. Details of HAZ surface fracture, a) pre-crack and propagation, b) striations in propagation zone and c) propagation and failure zone.

Details of surface fractures of the base metal, weld metal and HAZ can be seen in Figures 9-11. Figure 9a, shows the crack propagation along the grain boundaries of the base metal (rolling direction) without visible striations formation. The transition between propagation crack and failure zone of base metal is presented in Figure 9b, which is characterized by a combination of ductility (dimples) and cleavage. In contrast, some similarities can find in the surface fracture propagation of the weld metal and HAZ, as striations formation which present local variations on its distribution. Finally, we can observe that there is not similitude between failure zone of the weld metal and HAZ. In the first case the final rupture is caused by the overload with very little deformation. However, in the second case the failure zone has been delimitated by a transition between cleavage (fatigue crack) and dimples (overload crack).

4. CONCLUSION

The experimental results reported in this work provide the means to observe and quantify the effect of fatigue crack growth on 6061-T6 aluminum alloy welds obtained by MIEA. In this context, it has been observed that mechanical properties and microstructural conditions have a very important effect on crack growth. These conditions present a critical point in terms of the stress intensity factor ~ 15 MPa $m^{1/2}$. It means that under this value the crack growth of the base metal are faster than weld metal and HAZ. However above this value the weld metal has the worst conditions (crack growth), followed by HAZ and base metal (6061-T6).

5. REFERENCES

[1] Gladman T. *Precipitation Hardening in Metals, Materials Science and Technology*, vol. 15, pag. 30-36, 1999.

[2] Gupta A.K, Lloyd D.J and Court SA. *Precipitation hardening in Al–Mg–Si alloys with and without excess Si*. Materials science and engineering A, 316, pag. 11-17 2001.

[3] Malin V. *Study of metallurgical phenomena in the HAZ of 6061-T6 aluminium welded joints*. Welding Journal 1995; vol. 74: 305s-18s.

[4] Ambriz R.R, Barrera G, Garcia R and Lopez V.H. *A Comparative Study of the Mechanical Properties of 6061-T6 GMA Welds Obtained by the Indirect Electric Arc (IEA) and the Modified Indirect Electric Arc (MIEA)*. Materials and Design, vol. 30, pag. 2446-2453, 2009.

[5] Ambriz R.R, Gerardo Barrera, Rafael García and López VH. Microstructure and Heat Treatment Response of 2014-T6 GMAW Welds Obtained with a Novel Modified Indirect Electric Arc Joint. Soldagem and Inspecao 2008; vol. 13: 255-63.

[6] R.R. Ambriz, Mesmacque G, Ruiz A, Amrouche A and López V.H. *Effect of the welding profile generated by the modified indirect electric arc technique on the fatigue behavior of 6061-T6 aluminum alloy*. Materials science and engineering A, in press, 2009.

[7] Ambriz R.R, Barrera G and García R. *Aluminum 6061-T6 Welding by Means of the Modified Indirect Electric Arc Process*. Soldagem and Inspecao, vol. 11, pag. 10-17, 2006.

[8] ASM. Properties and Selection: *Nonferrous Alloys and Special-Purpose Materials*, 1992.

[9] Myhr O.R, Grong O, Fjaer H.G and Marioara C.D, *Modelling of the Microstructure and Strenght Evolution in Al-Mg-Si Alloys During Multistage Thermal Processing*. Acta Materialia, vol 54, pag. 4997-5008, 2004.

[10] Dutta I and Allen S.M. *Calorimetric Study of Precipitation in Comercial Al Alloys*. Journal of Materials Science Letters, vol 10, pag. 323-326, 1991.